

Electrochemical CO Reduction Builds Solvent Water into Oxygenate Products

Yanwei Lum,^{†,‡,⊥} Tao Cheng,^{§,||,⊥} William A. Goddard, III,^{*,§,||,⊥} and Joel W. Ager^{*,†,‡,⊥}

[†]Joint Center for Artificial Photosynthesis and Materials Sciences Division, Lawrence Berkeley National Laboratory, Berkeley, California 94720, United States

[‡]Department of Materials Science and Engineering, University of California, Berkeley, California 94720, United States

[§]Joint Center for Artificial Photosynthesis, California Institute of Technology, Pasadena, California 91125, United States

^{||}Materials and Process Simulation Center (MC139-74), California Institute of Technology, Pasadena, California 91125, United States

Supporting Information

ABSTRACT: Numerous studies have examined the electrochemical reduction of CO (COR) to oxygenates (e.g., ethanol). None have considered the possibility that oxygen in the product might arise from water rather than from CO. To test this assumption, C¹⁶O reduction was performed in H₂¹⁸O electrolyte. Surprisingly, we found that 60–70% of the ethanol contained ¹⁸O, which must have originated from the solvent. We extended our previous all-solvent density functional theory metadynamics calculations to consider the possibility of incorporating water, and indeed, we found a new mechanism involving a Grotthuss chain of six water molecules in a concerted reaction with the *C–CH intermediate to form *CH–CH(¹⁸OH), subsequently leading to (¹⁸O)ethanol. This competes with the formation of ethylene that also arises from *C–CH. These unforeseen results suggest that all previous studies of COR under aqueous conditions must be reexamined.

Electrochemical CO₂ reduction (CO₂R) has emerged as a promising technology to utilize increasingly cheaper renewable electricity to convert CO₂ into useful chemicals and fuels.^{1–6} In this context, Cu-based catalysts are currently the most promising for driving CO₂R to produce significant amounts of multicarbon oxygenates and hydrocarbons such as ethanol and ethylene.^{7–10} Enabling the deterministic design of more selective and efficient catalysts requires understanding of the reaction mechanisms to predict how changes in the catalysts and electrolyte can modify the kinetics and products. Indeed, a number of theoretical papers have been published explaining how the experimentally observed changes in products depend on the pH, applied potential, and presence of counterions.^{11–14} It is generally accepted that on various Cu surfaces, CO₂ is first reduced to CO.^{15,16} At low pH, CO can be further reduced to *COH or *CHO and then to *CH₂OH, leading to methane or methanol formation.^{14,17} At pH > 7, CO can undergo C–C coupling to generate a *CO–CO dimer,^{14,17–21} which then forms *OC–COH.²² Subsequent steps leading to ethylene and ethanol have been further studied in quantum mechanics (QM)-based theory papers.^{17–19,23–25}

Recently, we published the first complete determination of the atomistic reaction mechanism for CO reduction (COR) on Cu(100) using QM-based metadynamics in full solvent to determine the free energy barriers and kinetics at 298 K.¹⁸ We showed that solvent water on the Cu surface plays an essential role in the mechanisms by providing hydrogen to the intermediates and products. This role of surface water, which involves transferring hydrogen to these intermediates, often through a Grotthuss mechanism involving other solvent waters, was a new result. In our previous QM calculations¹⁸ on CO reduction on Cu, we found that the pathway for ethanol formation proceeds through *(OH)C–CH, an intermediate formed after four electron transfers, which is then subsequently reduced either to *C–CH (leading to ethylene formation with a free energy barrier of 0.61 eV) or to *H(OH)C–CH (leading to ethanol formation with a free energy barrier of 0.67 eV). However, we did not consider the possibility that solvent water could provide the oxygen in the products, and we assumed that all of the O atoms in the oxygenate (C_nH_mO_x) products come from the original CO molecule being reduced. In fact, this is a common feature of all current proposed mechanisms, with recent work by Head-Gordon and co-workers predicting that none of the oxygenate products should possess oxygen from the solvent water.²³

We tested this critical assumption experimentally by carrying out reduction of C¹⁶O in H₂¹⁸O electrolyte on oriented Cu surfaces and quantifying the isotopic composition of the products using gas chromatography–mass spectrometry (see the Supporting Information (SI) for more details). An important reason that COR and not CO₂R was performed is because CO₂ is known to rapidly equilibrate with water to form bicarbonate.²⁶ Therefore, dissolved CO₂ would likely incorporate ¹⁸O from the solvent, resulting in ¹⁸O in the products. In contrast, CO does not exchange O with water (see the SI for more details). The reduction of C¹⁶O in 0.05 M K₂CO₃ electrolyte (pH 11.3) was carried out with different Cu orientations, namely, Cu(111), Cu(100), and Cu(751), at a potential of –0.64 V vs RHE. Analysis of the isotopic composition of the products (Figure 1a) revealed that the

Received: April 13, 2018

Published: July 16, 2018



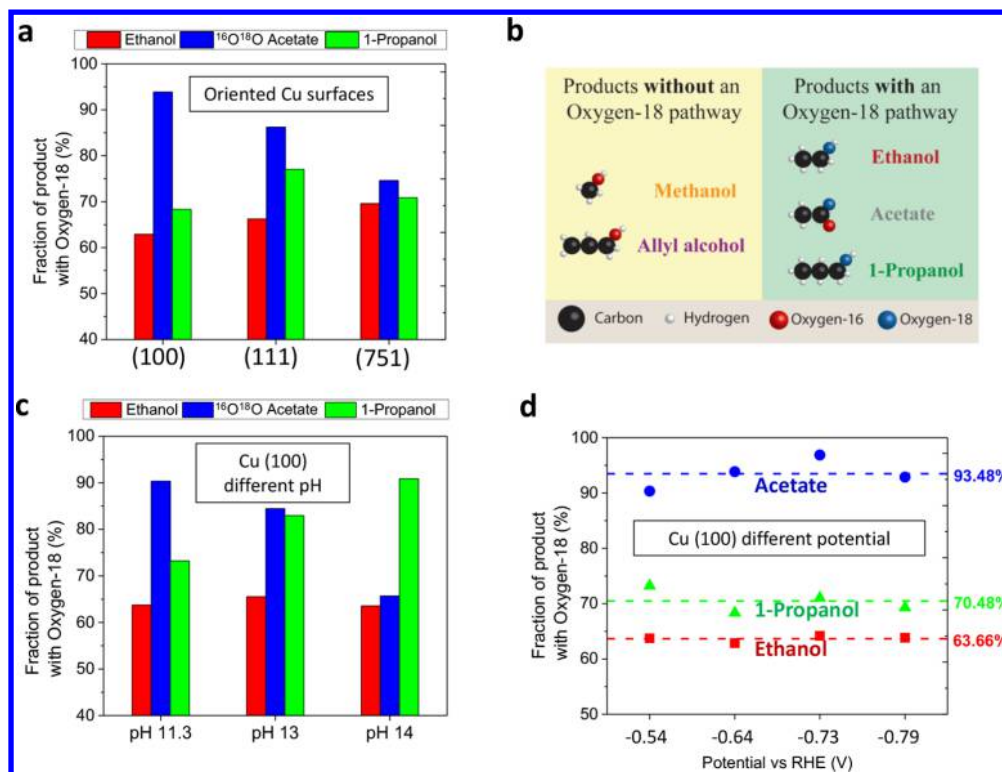


Figure 1. Fractions of ethanol (red), acetate (blue), and 1-propanol (green) products containing ^{18}O for C^{16}O reduction in H_2^{18}O electrolyte (a) on Cu with different orientations tested at ca. -0.65 V vs RHE, (c) on Cu(100) at different pH, and (d) on Cu(100) at different applied potentials. (b) Chart showing products with an ^{18}O pathway (ethanol, acetate, and 1-propanol) and products without an ^{18}O pathway (methanol and allyl alcohol). Note: ($^{18}\text{O}^{18}\text{O}$)acetate was never observed as a product. Faradaic efficiency data are available in the SI.

majority of the ethanol, acetate, and 1-propanol were ^{18}O -enriched. In order to ensure that incorporation of ^{18}O into the products was not solely due to homogeneous reactions occurring in the bulk of the electrolyte (e.g., Cannizzaro reactions²⁷), a series of control experiments were conducted (see the SI for more details). Control experiments were also performed to ensure that the mass spectrometer had similar detection sensitivities for ^{16}O and ^{18}O fragments (see the SI for more details).

For all three Cu surfaces, the fraction of ethanol with ^{18}O was around 66%, and that for 1-propanol was around 72%. Acetate possesses two oxygen atoms and therefore may have three different configurations: ($^{16}\text{O}^{16}\text{O}$)-, ($^{16}\text{O}^{18}\text{O}$)-, and ($^{18}\text{O}^{18}\text{O}$)acetate. ($^{18}\text{O}^{18}\text{O}$)acetate was not observed on any of the Cu surfaces, and the distribution of $^{16}\text{O}^{16}\text{O}$ versus $^{16}\text{O}^{18}\text{O}$ depended on the Cu orientation, with Cu(100) producing the highest fraction of $^{16}\text{O}^{18}\text{O}$ ($>90\%$). Additionally, allyl alcohol (prop-2-en-1-ol) was detected as a product on all of the surfaces and methanol only on the Cu(111) surface. Interestingly, allyl alcohol and methanol were not enriched with ^{18}O , which suggests that the mechanisms for their formation may be very different. These findings are summarized in the chart in Figure 1b, which sorts the products into those with ^{18}O and those without ^{18}O .

Next, the effects of pH and potential were investigated for the Cu(100) surface. A potential of around -0.53 V vs RHE was applied at different pH: 11.3 (0.05 M K_2CO_3), 13 (0.1 M KOH), and 14 (1.0 M KOH). Figure 1c shows that changing the pH had no effect on the ^{18}O composition of ethanol, which remained at around 64%. On the other hand, the ^{18}O compositions of acetate and 1-propanol were significantly

affected by pH. For 1-propanol, the ^{18}O content increased from 73% at pH 11.3 to 91% at pH 14. However, for acetate, the $^{16}\text{O}^{18}\text{O}$ content decreased from 90% at pH 11.3 to 66% at pH 14. Keeping the pH constant at 11.3 and changing the potential (Figure 1d) had no effect on the isotopic composition of the products. Additionally, changing the potential and pH did not result in any $^{18}\text{O}^{18}\text{O}$ acetate formation.

To summarize the experiments, by using ^{18}O labeling of the solvent we have discovered that the majority of the ethanol, acetate, and 1-propanol molecules produced by COR on single-crystal Cu surfaces possess ^{18}O , showing conclusively that solvent water plays a dominant role in their formation. As a result of this unexpected finding, all previous mechanisms for the formation of $\text{C}_n\text{H}_m\text{O}_x$ oxygenates require reexamination because H_2O as the dominant source of O for the formation of these products has been overlooked.

Stimulated by the experimental results, we used QM-based metadynamics with full solvent (five layers) to determine the free energy barriers at 298 K in order to investigate how solvent H_2^{18}O could contribute ^{18}O to the product. The experimental results clearly demonstrate the existence of two ethanol formation pathways (an ^{16}O pathway and an ^{18}O pathway). Therefore, H_2^{18}O must react with a C_2 intermediate that has lost both of its oxygen atoms: either $^*\text{C}-\text{CH}$, $^*\text{C}-\text{CH}_2$, or $^*\text{HC}-\text{CH}_2$. We considered that the most plausible C_2 intermediate to react with H_2^{18}O is adsorbed ethynyl ($^*\text{C}-\text{CH}$). Thus, we explored the possibility of two-step $^*\text{CH}-\text{CH}(\text{OH})$ formation:

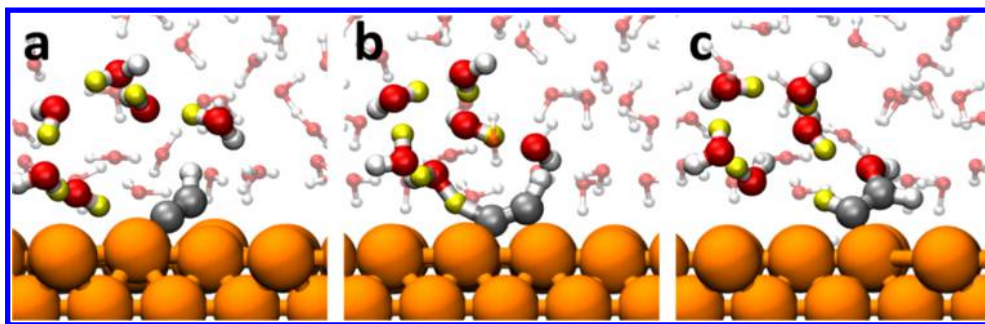


Figure 2. Reactive trajectory for Grotthuss chain ethynyl concerted hydrolysis (GECH) of $*C-CH$ to $*CH-CH(OH)$ from full-solvent QM molecular metadynamics free energy calculations: (a) initial reactants; (b) transition state (free energy barrier = 0.81 eV); (c) final products (exothermic by -0.12 eV). All six waters in the Grotthuss chain are shown in full. The other 48 water molecules not involved in the chain have been faded out for clarity. The colors are C in gray, O in red, H involved in the Grotthuss chain proton transfer in yellow, and other H in white. The intermediate $CH-CH(OH)$ formed by GECH subsequently forms ethanol, as shown in the orange pathway in Figure 3. We examined a number of possible pathways involving various numbers of waters, and this was the most favorable one.

1. First, one surface $H_2^{18}O$ might provide H^+ to form $*HC-CH$ plus surface ^{18}OH ($*^{18}OH$) via proton-coupled electron transfer (PCET).
2. Second, this might be followed by extraction of H^+ from a solvent $H_2^{18}O$ by $*^{18}OH$ to deliver the ^{18}OH to form $*CH-CH(^{18}OH)$ via PCET.

However, the free energy barrier for the first step is 1.09 eV, while that for the second step is 1.22 eV. These barriers are much larger than the values of 0.61 and 0.67 eV that we found previously to produce ethene and ethanol. Thus, we conclude that this mechanism does not explain the large amount of ^{18}O ethanol observed.

We then investigated a concerted pathway of water addition reaction via Grotthuss water chain in which the water at the C end provides H^+ to C (in $*C-CH$) while the water at the CH end simultaneously provides $^{18}OH^-$ to CH (in $*C-CH$), with these two waters being connected by a hydrogen-bonding network through bridging water molecules. We considered several possible such chains and found that the best involves six water molecules, leading to a reaction free energy barrier for this reaction of 0.81 eV. We also examined this reaction for chemisorbed ethyne ($*HC-CH$) to form $*CH_2-CH(^{18}OH)$ and found a slightly higher barrier of 0.84 eV. Finally, we also examined the reaction in which $*C-CH$ (ethynyl) forms $*C(^{18}OH)H-CH$ and found a barrier of 0.91 eV. Thus, we distinguish the formation of $*CH-CH(^{18}OH)$ from $*C-CH$ via water addition as the most possible mechanism contributing to $C_2H_5(^{18}OH)$ formation. We refer to this most unexpected and unprecedented reaction, which has not been reported previously, as Grotthuss chain ethynyl concerted hydrolysis (GECH). The critical steps of this unprecedented non-electrochemical reaction from QM-based metadynamics snapshots are shown in Figure 2 (also see the [supplementary movie](#)).

After the formation of $*CH-CH(^{18}OH)$ from $*C-CH$ via water addition, the remaining steps leading to $C_2H_5(^{18}OH)$ formation and the related energetics are as shown in Figure 3. GECH is expected to be independent of pH and applied potential. In the SI, we report a simulation with explicit consideration of 1 M NaOH (pH 14), where we found a free energy barrier of 0.87 eV, supporting this claim. The experimental results in Figure 1c,d do not show a large dependence on either pH or potential, supporting our claim that GECH is responsible for the formation of ^{18}O ethanol.

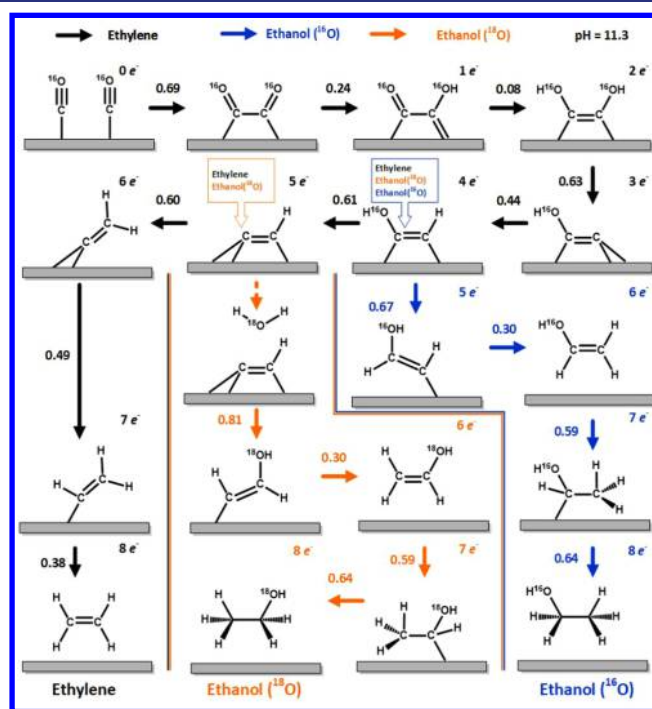


Figure 3. Mechanistic pathways for CO reduction predicted from full-solvent QM-based molecular metadynamics to obtain free energy reaction barriers at 298 K. The pathways for the formation of ethylene (black) and (^{16}O) ethanol (blue) are from ref 18. The (^{18}O) ethanol formation pathway (orange) is a newly discovered mechanism (GECH) reported here.

Since $*(^{16}OH)C-CH$ is a common intermediate for forming either (^{16}O) ethanol or ethylene + (^{18}O) ethanol (see Figure 3), the predicted energy barriers at 298 K (0.67 and 0.61 eV, respectively) can be used to estimate the ratio of ethylene + (^{18}O) ethanol to ^{16}O ethanol. On the basis of the Arrhenius equation, this ratio was calculated to be 11, in excellent agreement with our experiments, which yielded a ratio of 14 and a calculated energy difference in barriers of 0.066 eV (see Figure S28 for calculation details). Similarly, $*C-CH$ is a common intermediate for forming both (^{18}O) ethanol and ethylene, and the predicted activation energies at 298 K (0.81 and 0.61 eV) can be compared to the observed ratio of 0.15, which implies that the difference in barriers is 0.049 eV. This difference in experiment and theory

suggests that we may not have exhausted all of the pathways for the GECH mechanism.

In summary, our QM-based metadynamics calculations show that (^{18}O)ethanol results from solvent-based concerted hydrolysis by $^*\text{C}-\text{CH}$ (chemisorbed ethyne) to form $^*\text{CH}-\text{CH}(\text{OH})$, in which the added H and OH are derived from waters at the opposite ends of a six-molecule Grotthuss chain. This is a brand-new mechanism that is independent of pH and applied potential and may provide new approaches to the design of nanoscale structures and compositions in which the energy and orientation of the chemisorbed ethynyl intermediates are used to promote solvent-water-induced ethanol or other $\text{C}_n\text{H}_m\text{O}_x$ oxygenate products.

In this work, the main focus was to understand the formation of (^{18}O)ethanol was because it is the most abundant ^{18}O -containing oxygenate produced. Subsequent work will examine the C_3 product pathways for 1-propanol and allyl alcohol formation as well as the acetate pathways, which are evidently more complicated. Since we now know that incorporation of ^{18}O is critical in the formation of oxygenates, it is paramount to use this technique to investigate other catalyst systems used for COR, such as bimetallic systems and oxide-derived Cu.^{28–32} For example, oxide-derived Cu catalysts have been shown to yield a high selectivity toward oxygenates versus hydrocarbons.³¹ It is expected that such experiments will lead to new insights on how oxygenate formation mechanisms might be different on these catalysts. Finally, our discovery of concerted solvent water incorporation of O into oxygenates may have implications for many other oxygen insertion processes.

■ ASSOCIATED CONTENT

Supporting Information

The Supporting Information is available free of charge on the ACS Publications website at DOI: 10.1021/jacs.8b03986.

Synthesis, characterization, experimental methods, and control experiments (PDF)

Movie showing a reactive trajectory for the formation of $^*\text{CH}-\text{CH}(\text{OH})$ from $^*\text{C}-\text{CH} + \text{H}_2\text{O}$ (MPG)

■ AUTHOR INFORMATION

Corresponding Authors

*wag@wag.caltech.edu

*jwager@lbl.gov

ORCID

Tao Cheng: 0000-0003-4830-177X

William A. Goddard, III: 0000-0003-0097-5716

Joel W. Ager: 0000-0001-9334-9751

Author Contributions

[†]Y.L. and T.C. contributed equally.

Notes

The authors declare no competing financial interest.

■ ACKNOWLEDGMENTS

This material is based upon work performed by the Joint Center for Artificial Photosynthesis, a DOE Energy Innovation Hub supported through the Office of Science of the U.S. Department of Energy under Award DE-SC0004993. Y.L. acknowledges the support of an A*STAR National Science Scholarship. This work used the Extreme Science and Engineering Discovery Environment (XSEDE), which is

supported by National Science Foundation grant number ACI-1548562. We thank Lingfei Wei for assistance with technical illustrations.

■ REFERENCES

- (1) Hori, Y. In *Modern Aspects of Electrochemistry*; Vayenas, C. G., White, R. E., Gamboa-Aldeco, M. E., Eds.; Springer: New York, 2008; pp 89–189.
- (2) Montoya, J. H.; Seitz, L. C.; Chakthranont, P.; Vojvodic, A.; Jaramillo, T. F.; Nørskov, J. K. *Nat. Mater.* **2017**, *16*, 70.
- (3) Qiao, J.; Liu, Y.; Hong, F.; Zhang, J. *Chem. Soc. Rev.* **2014**, *43*, 631.
- (4) Chu, S.; Cui, Y.; Liu, N. *Nat. Mater.* **2017**, *16*, 16.
- (5) Graves, C.; Ebbesen, S. D.; Mogensen, M.; Lackner, K. S. *Renewable Sustainable Energy Rev.* **2011**, *15*, 1.
- (6) Singh, M. R.; Clark, E. L.; Bell, A. T. *Proc. Natl. Acad. Sci. U. S. A.* **2015**, *112*, E6111.
- (7) Hori, Y.; Murata, A.; Takahashi, R. *J. Chem. Soc., Faraday Trans. 1* **1989**, *85*, 2309.
- (8) Kuhl, K. P.; Cave, E. R.; Abram, D. N.; Jaramillo, T. F. *Energy Environ. Sci.* **2012**, *5*, 7050.
- (9) Kuhl, K. P.; Hatsukade, T.; Cave, E. R.; Abram, D. N.; Kibsgaard, J.; Jaramillo, T. F. *J. Am. Chem. Soc.* **2014**, *136*, 14107.
- (10) Kim, D.; Kley, C. S.; Li, Y.; Yang, P. *Proc. Natl. Acad. Sci. U. S. A.* **2017**, *114*, 10560.
- (11) Pérez-Gallent, E.; Marcandalli, G.; Figueiredo, M. C.; Calle-Vallejo, F.; Koper, M. T. M. *J. Am. Chem. Soc.* **2017**, *139*, 16412.
- (12) Resasco, J.; Chen, L. D.; Clark, E.; Tsai, C.; Hahn, C.; Jaramillo, T. F.; Chan, K.; Bell, A. T. *J. Am. Chem. Soc.* **2017**, *139*, 11277.
- (13) Resasco, J.; Lum, Y.; Clark, E.; Zeledon, J. Z.; Bell, A. T. *ChemElectroChem* **2018**, *5*, 1064.
- (14) Xiao, H.; Cheng, T.; Goddard, W. A.; Sundararaman, R. *J. Am. Chem. Soc.* **2016**, *138*, 483.
- (15) Hori, Y.; Takahashi, R.; Yoshinami, Y.; Murata, A. *J. Phys. Chem. B* **1997**, *101*, 7075.
- (16) Peterson, A. A.; Abild-Pedersen, F.; Studt, F.; Rossmeisl, J.; Nørskov, J. K. *Energy Environ. Sci.* **2010**, *3*, 1311.
- (17) Xiao, H.; Cheng, T.; Goddard, W. A. *J. Am. Chem. Soc.* **2017**, *139*, 130.
- (18) Cheng, T.; Xiao, H.; Goddard, W. A. *Proc. Natl. Acad. Sci. U. S. A.* **2017**, *114*, 1795.
- (19) Calle-Vallejo, F.; Koper, M. T. M. *Angew. Chem., Int. Ed.* **2013**, *52*, 7282.
- (20) Sandberg, R. B.; Montoya, J. H.; Chan, K.; Nørskov, J. K. *Surf. Sci.* **2016**, *654*, 56.
- (21) Goodpaster, J. D.; Bell, A. T.; Head-Gordon, M. *J. Phys. Chem. Lett.* **2016**, *7*, 1471.
- (22) Pérez-Gallent, E.; Figueiredo, M. C.; Calle-Vallejo, F.; Koper, M. T. M. *Angew. Chem., Int. Ed.* **2017**, *56*, 3621.
- (23) Garza, A. J.; Bell, A. T.; Head-Gordon, M. *ACS Catal.* **2018**, *8*, 1490.
- (24) Luo, W.; Nie, X.; Janik, M. J.; Asthagiri, A. *ACS Catal.* **2016**, *6*, 219.
- (25) Nie, X.; Esopi, M. R.; Janik, M. J.; Asthagiri, A. *Angew. Chem., Int. Ed.* **2013**, *52*, 2459.
- (26) Wang, X.; Conway, W.; Burns, R.; McCann, N.; Maeder, M. J. *Phys. Chem. A* **2010**, *114*, 1734.
- (27) Birdja, Y. Y.; Koper, M. T. M. *J. Am. Chem. Soc.* **2017**, *139*, 2030.
- (28) Ma, S.; Sadakiyo, M.; Heima, M.; Luo, R.; Haasch, R. T.; Gold, J. I.; Yamauchi, M.; Kenis, P. J. A. *J. Am. Chem. Soc.* **2017**, *139*, 47.
- (29) Ren, D.; Ang, B. S.-H.; Yeo, B. S. *ACS Catal.* **2016**, *6*, 8239.
- (30) Kim, D.; Resasco, J.; Yu, Y.; Asiri, A. M.; Yang, P. *Nat. Commun.* **2014**, *5*, 4948.
- (31) Li, C. W.; Ciston, J.; Kanan, M. W. *Nature* **2014**, *508*, 504.
- (32) Roberts, F. S.; Kuhl, K. P.; Nilsson, A. *Angew. Chem.* **2015**, *127*, 5268.